Computers and Electronics in Agriculture 118 (2015) 47–55

Contents lists available at ScienceDirect

Computers and Electronics in Agriculture

journal homepage: www.elsevier.com/locate/compag

Mosquito vector monitoring system based on optical wingbeat classification

Tai-Hsien Ouyang [a], En-Cheng Yang [b,c], Joe-Air Jiang [a], Ta-Te Lin [a,c,*]

[a] Department of Bio-Industrial Mechatronics Engineering, National Taiwan University, Taiwan, ROC
[b] Department of Entomology, National Taiwan University, Taiwan, ROC
[c] Graduate Institute of Brain and Mind Sciences, National Taiwan University, Taiwan, ROC

ARTICLE INFO

Article history:
Received 4 May 2015
Received in revised form 19 August 2015
Accepted 19 August 2015

Keywords:
Mosquito
Disease vector
Population monitoring
Gaussian mixture model

ABSTRACT

We developed an automatic mosquito classification system which consists of an infrared recording device for profiling the wingbeat of the in-flight mosquito species and a machine learning model for classifying the gender, genus, and species of the incoming mosquitoes by the signatures of their wingbeats.

The recording device is a set of infrared emitters and receivers, which are attached to the wall of an apparatus. When the winged subject enters the apparatus, its flapping wings block the infrared beam from the emitters intermittently such that the receivers convert the wingbeat to the electrical waveform. To classify the incoming subjects, we proposed a machine learning method, which is the Gaussian mixture model trained using the expectation-maximization algorithm (EM-GMM), and compared it with the previously proposed algorithms, including the artificial neuron network model (ANN) and the nearest neighbor model.

To assess the performance of the system, we used the living male and female *Aedes albopictus*, *Aedes aegypti* and *Culex quinquefasciatus*. The results show that the accuracies of the proposed system are above 80% on identifying the gender and genus of the mosquitoes, with the precisions above 80% and 70%, respectively. The results also suggest that the EM-GMM algorithm outperforms the other two algorithms on the accuracy and precision of the classification of the classes of mosquitoes. In addition to the evaluation of the performance of the system, we also found that certain classes of mosquitoes share similar wingbeat characteristics, which implies that the distinctive wingbeat characteristics should be considered for the optimal accuracy of the classification of the insects of interest.

1. Introduction

Preventing humans, poultry, or livestock from mosquito-borne diseases reduces the economic losses which are caused by the disease infections. *Aedes* mosquitoes are important vectors of zoonotic arbovirus, including West Nile virus, yellow fever, dengue fever, and encephalitis (Gubler, 1989; Gubler and Clark, 1996; Eritja et al., 2005). In addition, filarial diseases transmitted by *Culex* are not only infectious to humans but also to buffalos, goats and sheep. While infection might cause an increase in medical expenses and a reduction of livestock production, effective mosquito control programs rely on statistical indices based on mosquito population monitoring. The conventional approach used for mosquito population monitoring is based on ovitraps, whose advantages are low-cost and convenience of deployment, but they suffer from low sampling frequency (Zeichner and Perich, 1999; Polson et al., 2002; Lenhart et al., 2005).

Some previous approaches applied to detecting and monitoring insect movements were based on wingbeat (Reynolds and Riley, 2002). The characteristics of mosquito wingbeat were studied through acoustic, optical, and radar approaches (Landois, 1867; Chadwick, 1939; Reed et al., 1942; Sotavalta, 1952; Jones, 1964; Belton and Costello, 1979; Unwin and Ellington, 1979; Moore, 1991; Mankin, 1994; Moore and Miller, 2002; Riley and Smith, 2002; Reynolds and Riley, 2002; Li et al., 2005; Pennetier et al., 2010), but there are certain difficulties for implementing a robust system for in-field mosquito population monitoring using these methods. On the measuring instrument for the features of mosquito wingbeats, the frequency of the wingbeats was measured using tuning forks in the early stage of this field of research (Landois, 1867; Sotavalta, 1952), a procedure which lacks quantitative precision and objectivity. Later, microphones were introduced in acoustic approaches, but microphones suffer from

* Corresponding author at: Department of Bio-Industrial Mechatronics Engineering, National Taiwan University, No. 1, Roosevelt Rd., Sec. 4, Taipei 10617, Taiwan, ROC. Tel.: +886 2 33665331; fax: +886 2 23929416.

E-mail address: m456@ntu.edu.tw (T.-T. Lin).

http://dx.doi.org/10.1016/j.compag.2015.08.021
0168-1699/

the inconvenience of sound-proof instruments (Williams and Galambos, 1950; Jones, 1964), although acoustic approaches have been widely used in studies on behavior related to insects' auditory organs (Johnston, 1855; Mankin, 1994; Göpfert and Robert, 2001; Gibson and Russell, 2006; Jackson and Robert, 2006; Robert, 2009; Cator et al., 2009). On the other hand, optical approaches were also proposed. Early studies used the stroboscopic approach to measure the changes of light intensity created by the wingbeat of insects (Chadwick, 1939; Williams and Galambos, 1950). More recently, experiments were performed using photo sensors working in a spectrum range, which provided more adequate signals within a spectrum range, which provides better signal-to-noise ratio (SNR) than the acoustic methods (Unwin and Ellington, 1979; Moore et al., 1986; Byrne et al., 1988; Riley, 1989; Oertli, 1989). Cameras were also introduced in the research on insect flight kinematics (Ellington, 1984; Hardie and Powell, 2002) and swarming (Ikawa et al., 1994), but due to the tiny size of the study subject, the optical methods suffer from the resolution of the sensor. Radar approaches were used in remote sensing of insect migration; the insects could be distinguished from other objects by the radar-derived wingbeat frequency. However, insect identification for intra-species was difficult due to the overlapped frequency distributions of the radar returns (Riley, 1989; Riley and Smith, 2002). Concerning the tools for analysis, spectral characteristics of wingbeat were used to identify insect species. The primitive approaches for identifying mosquito wingbeats relied heavily on researchers' absolute pitch (Landois, 1867) or accurate oscilloscopic records converted from acoustic signals (Williams and Galambos, 1950). With the rapid progress of computers, automatic classification algorithms were introduced in the studies on insect wingbeat. Artificial Neural Network (ANN) classifiers, for example, were introduced to automatically identify in-flight mosquitoes through spectral wingbeat characteristics (Moore, 1991; Li et al., 2005). Research papers on the identification of assorted insect species using different algorithms were proposed, but some mosquito species shared similar wingbeat frequencies (Moore, 1991; Moore and Miller, 2002; Li et al., 2005). Therefore, a system with a high-resolution measurement tool which is robust to the environmental noise and the corresponding tools for analysis for mosquito wingbeats has yet to be developed and is needed for the research on mosquito wingbeats and for large-scale vector monitoring.

To address the challenges mentioned above, we propose a mosquito classification system that consists of an infrared sensor array recording device, a set of software programs based on a classification algorithm, and a method that can be trained to identify *Aedes albopictus*, *Aedes aegypti* and *Culex quinquefasciatus* when they are in flight. The spiral infrared sensor array recording device proposed in this paper provides robustness to the environmental noise, and the structure is simple enough for large-scale deployment. The recorded wingbeat data are transformed into cepstrum to improve the identification performance of mosquito wingbeat (Moore and Miller, 2002). Then the Gaussian Mixture Model-based (GMM) classifier, which have been widely applied to human voice identification, is introduced in this research (Gish and Schmidt, 1994; Gauvain and Lee, 1994; Reynolds, 1995; Kinnunen et al., 2006). The proposed method is tested with experiments in classifying three mosquito species: *A. albopictus*, *A. aegypti* and *C. quinquefasciatus*, and their gender, based on the recorded optical wingbeat sequences.

2. Materials and methods

2.1. Mosquito colonies

Colonies of the three mosquito species: *A. albopictus*, *A. aegypti* and *C. quinquefasciatus*, were collected from Taipei City, Taiwan, and were raised and maintained by feeding the 5% sucrose solution in growth chambers under constant environmental conditions (Temp. = 25 °C, RH > 80%). The evaluation group consisted of 745 optical wingbeat sequences from 120 mosquitoes ($n = 120$, 20 individuals for each gender of the 3 species) and the training group consisted of 43 sequences from 12 mosquitoes. ($n = 12$; at least 2 individuals for each gender of the 3 species). The duration of extracted sequences ranged from 50 to 100 ms.

2.2. Infrared-based wingbeat sensor

The wingbeat recording device consists of three infrared emitters and the corresponding receivers (working wavelength = 830 nm). The pairs of emitters and receivers were arranged in a double helix pattern and attached to the observation apparatus (Fig. 1). The observation apparatus was made with a 15 ml conical polypropylene tube. In this research, the apparatus was closed-ended; it can be open-ended or closed-ended when being attached to the mosquito trap. The emitters and receivers were wired in parallel. Thus, the emitters and receivers formed three pairs of photo-interrupters. The receivers were powered by a 6 V DC power supply from the data acquisition card, and the emitters were powered by 6 V battery. Mosquitoes' flying directions and environmental lighting conditions were not under control during the experiments.

2.3. Wingbeat signal acquisition and processing

In each experiment, one mosquito was manually transferred into the observation apparatus to conduct wingbeat recording. The wingbeat waveform was recorded in the observation

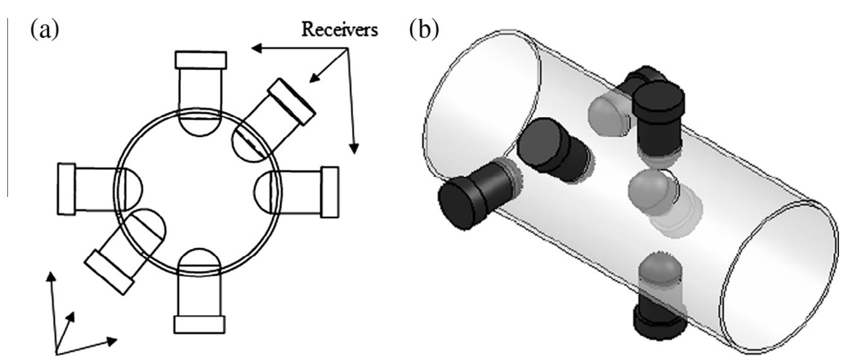

Fig. 1. The optical wingbeat recording device. The diagrams present (a) the configuration of the double helix arrangement of the transmitters and receivers, and, (b) the rendered sketch of the optical wingbeat recording device.

apparatus for 20 s at a 5000 Hz sampling frequency. Each mosquito's wingbeat sequence was manually extracted using the audio editing software GoldWave 5.58 (GoldWave, Newfoundland, Canada). In order to ensure the quality of the dataset, the wingbeat sequences with at least 50 ms duration and above ±0.1 V amplitude were collected for each mosquito. To eliminate the noise from power lines, the recorded sequences were filtered by a 10-order Butterworth high-pass filter with the cut-off frequency of 60 Hz.

The receivers of photo-interrupters were connected to the data acquisition card PCI-6013 (National Instrument, Austin, TX) which was installed in a personal computer equipped with Core 2 Duo E8400 3.0 GHz CPU (Intel, Santa Clara, CA) and 4.0 GB RAM. Software programs in this research were developed with MATLAB 2006b (Mathworks, Natick, MA) and VOICEBOX (a speech processing toolbox for MATLAB, released by the Department of Electrical and Electronic Engineering, Imperial College, London, UK, under terms of the GNU License).

2.4. Model estimation and classification algorithms

To obtain the wingbeat frequency distribution as the features, the raw sequences were converted into cepstra by taking the inverse Fourier transform of the logarithm of the absolute value of the Fourier transform of the signal (Atal, 1974); the sequences were then converted into the 12-coefficient feature vectors by dividing the relative power on the cepstrum into 12 bins for the Gaussian mixture model estimation using the Expectation-Maximization algorithm (EM-GMM) (Reynolds, 1995). The probabilistic model of the mosquito wingbeat, i.e. θ, was described as a Gaussian mixture model with the weighted sum of M components of Gaussian distributions:

$$\theta = \sum_{i=1}^{M} w_i \frac{e^{-\frac{1}{2}(x-\mu_i)^T \sum_i^{-1}(x-\mu_i)}}{\sqrt{(2\pi)^d |\sum_i|}} \tag{1}$$

In Eq. (1), x is a data point, d is the dimension of the samples, w_i is the weight of component i, μ_i is the mean vector and $\sum_i$ is the covariance matrix of the Gaussian density function. To classify mosquitoes by their species and gender, a classification algorithm was developed in this research. For a sampled sequence $X = \{x_1, \ldots, x_T\}$ in the evaluation group, the classification algorithm identifies the most likely mosquito wingbeat model for the sequence (Reynolds, 1995) The classification algorithm is described by:

$$\hat{\theta} = \arg\max L(\theta|X) \tag{2}$$

In Eq. (2), $\hat{\theta}$ is the most likely model estimate, and $L(\theta|X)$ represents the likelihood of being model θ by sequence X. In the evaluation session, the posterior probability of each sample from the evaluation group to each model was calculated, and the candidate with the highest posterior probability was reported as the classified mosquito group. In building the wingbeat model θ, the wingbeat feature vectors were applied to the training program based on the expectation maximization (EM) algorithm (Dempster et al., 1977; Reynolds and Rose, 1995) developed with MATLAB. The EM algorithm iteratively estimates the parameters for a model using the estimates reached in the previous iteration until the threshold is achieved. The EM algorithm consists of two parts: estimation and maximization. In the estimation part, the expectation of the likelihood of a hidden value z with the probabilistic model θ_n and the data X was calculated. Then in the maximization part, the probabilistic model θ_{n+1} would be optimized. Therefore, the EM algorithm could be summarized as:

$$\theta_{n+1} = \arg\max_{\theta} \sum P(\theta_n, z|X) \tag{3}$$

Therefore, by running the EM algorithm, the weights of the Gaussian mixture model of the mosquito wingbeat were estimated.

In summary, each clip of the recorded wingbeat waveform is transformed into a cepstrum. Then, in the training session, the weights of the Gaussian mixture model, which is used in the classification session, were estimated with the EM algorithm. In the classification session, the likelihood of a sequence belonging to a class of mosquitoes was calculated. Therefore, the classification of a mosquito was determined (Fig. 2). The signal processing procedure of the system is presented in Fig. 2b. The wingbeat recording part converted the wingbeat of a flying mosquito into an analog electrical signal, and the data acquisition card converted the signal into a digital signal. Then, the cepstrum transformation was conducted in the signal processing part to extract the characteristics presented in the cepstrogram for classification. Finally, in the classification session, the posterior probability of each sample to each candidate model was calculated and the candidate model with the highest probability was reported as the classified group.

To compare the performances of the classification method and the methods which were proposed previously (Moore, 1991; Moore and Miller, 2002; Li et al., 2005), we implemented a classification program based on a two-layer feed-forward probabilistic artificial neural network algorithm (ANN) using the *newpnn* function in MATLAB. We also implemented the nearest neighbor algorithm (NN) as an alternative algorithm for the performance evaluation. The NN algorithm classifies the incoming mosquitoes by finding the model sequence which yields the highest Pearson correlation to the incoming wingbeat sequence.

2.5. Statistical analysis and performance evaluation

In order to ensure that the difference of estimated models between groups was significant so that the classification could be successfully achieved, the experimental data were analyzed by two-way ANOVA on every two groups of mosquitoes. Species and 12-cepstrum coefficients were considered as the two factors.

The classification performances of the algorithms are analyzed using the number of the true positives, the true negatives, the false positives, and the false negatives of the classification results. The merits of the methods are shown by the accuracy and the precision. The accuracy of the classification is defined as the sum of true positives and true negatives divided by the total number of samples; the precision is defined as the true positive divided by the sum of the true positive and the false positive.

3. Results and discussion

3.1. Comparisons of wingbeat characteristics

After mosquito wingbeat signals were acquired via the sensor array recording device, each time-domain sequence was converted into a cepstrum. Then the EM algorithm was used to create the Gaussian mixture models using the sequences of the training group for further mosquito species and gender classification. Typical examples of cepstrograms are illustrated in Fig. 3.

To compare the wingbeat characteristics of the six groups, we performed two-way ANOVA statistical analysis. The purpose of the analysis was to determine whether the wingbeat characteristics differed between tested groups. Table 1 presents the results of the analysis. The p-values of each two groups were all less than 0.05, except for those of male *C. quinquefasciatus* and male *A. albopictus* ($p = 0.1367$). The p-value being larger than the threshold implies that the difference between the wingbeats of the groups is not significant. This fact suggests that

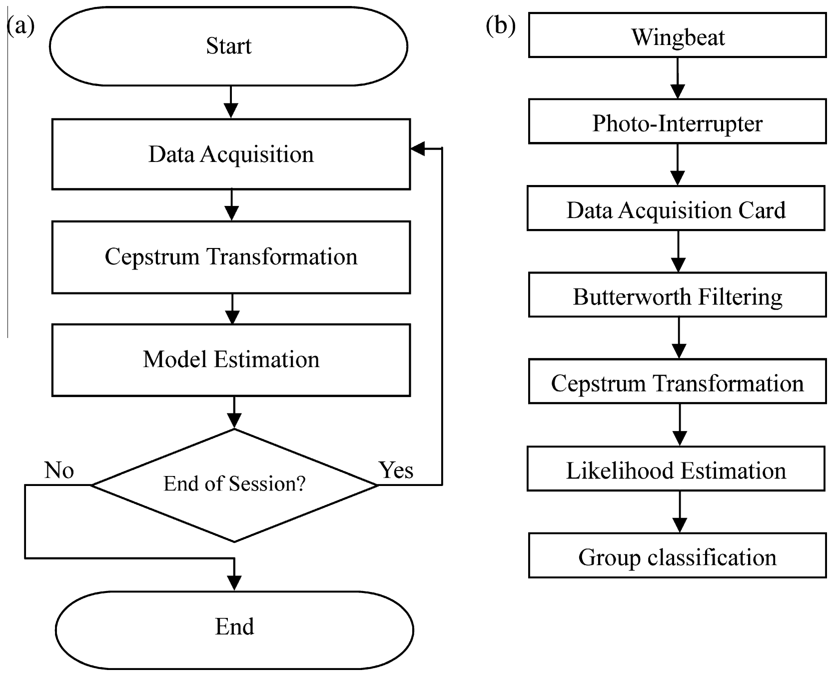

Fig. 2. The system architecture. (a) The flowchart of the system, including the training procedure using the EM-GMM method and classification procedure, (b) the system diagram of mosquito classification procedure.

it might not be feasible to differentiate the wingbeat patterns between male *C. quinquefasciatus* and male *A. albopictus* based on their cepstra. However, for the other 11 comparisons, the difference between each compared group appears to be significant. Therefore, it is promising to propose a method that classifies groups based on the significant difference in the cepstra of the groups.

To further compare the wingbeat characteristics of each test group, the 12 coefficients of the cepstra for all the samples of the six test groups are plotted in Fig. 4. Clusters of coefficients for test groups can be observed, and there are also overlapping parts. As shown in the ANOVA test results, the difference between the wingbeats of the male *C. quinquefasciatus* and male *A. albopictus* is not significant. Their cepstra coefficients are plotted in Fig. 5 for comparison. The distributions of the two groups are similar, corresponding to the results of the ANOVA test. By contrast, the coefficient distributions of other four groups (Fig. 4), demonstrate greater coefficient differences between groups compared to the distributions in Fig. 5.

3.2. Classification between gender and genus

Table 2 shows the comparison of the performance of the EM-GMM, ANN, and NN methods for gender classification. The classification accuracy of the EM-GMM method for the gender classification calculated from 745 samples is 87.9%, which is higher than the accuracies of the ANN method and the NN method, 86.0% and 80.3%, respectively. The true positive rates (the true positive divided by the sum of the true positive and the false negative) for male and female of the EM-GMM method, the ANN method, and the NN method are comparable, which are 76.1% and 98.0%, 71.1% and 98.8%, as well as 87.2% and 74.4%, respectively. As shown in Table 2, the precision of EM-GMM and ANN are particularly high on identifying the male mosquitoes, but the NN method performs better with the females.

Table 3 is the confusion matrix of the results of the inter-genus and gender classification experiments. The average accuracy of the EM-GMM method is 88.1%, which is still higher than the average accuracy of the ANN method and the NN method (80.1% and 76.1%, respectively). In this experiment, the precision of the EM-GMM method (73.6%) is much higher than the precision of the other two (59.2% and 47.1%).

Table 4 shows the performance of the three methods on classifying the six groups consisting of the 745 samples. The EM-GMM outperforms the ANN method and the NN method on accuracy and precision as well. Their accuracies are 85.5%, 79.5%, 73.4%, respectively. With regard to the true positive rate, EM-GMM and ANN yielded the lowest scores on *A. albopictus*, especially the male ones (0%, 6%, 19%, respectively), because they were classified as the male *A. aegypti*, For the precision of the three methods, the average precision of the three methods dropped to around 50%, but the precision of the EM-GMM method is still higher than the other two, and is the only one higher than 50%.

According to the confusion matrices shown in Tables 2–4, the EM-GMM method achieves the highest average accuracy and precision in the experiments. The suboptimal classification results of the male *A. aegypti* and *the* male *C. quinquefasciatus* can be explained by the absence of the significance of difference of the two classes, according to the ANOVA test. According to Fig. 3, male *A. aegypti* and male *C. quinquefasciatus* share similar wingbeat characteristics, which also explains the classification results between male *A. aegypti* and male *C. quinquefasciatus* in the confusion matrices.

Compared with the classification results which were presented in previous research that attempted to identify *A. aegypti, A. albopictus* and *C. quinquefasciatus* (Li et al., 2005), our EM-GMM method outperformed the ANN method on classifying *C. quinquefasciatus*, the female *A. aegypti*, and the female *A. albopictus.*

The confusion matrix of Table 4 also shows that species in the same genus (e.g. female *A. aegypti* and female *A. albopictus*) share similar wingbeat patterns, suggesting that the classification between two groups in the same genus would be challenging; this finding echoes the classification results previously reported (Li et al., 2005).

According to the results of the two-way ANOVA (Table 1), the means of the wingbeat frequency of male *C. quinquefasciatus* and male *A. albopictus* are not significantly different from each other

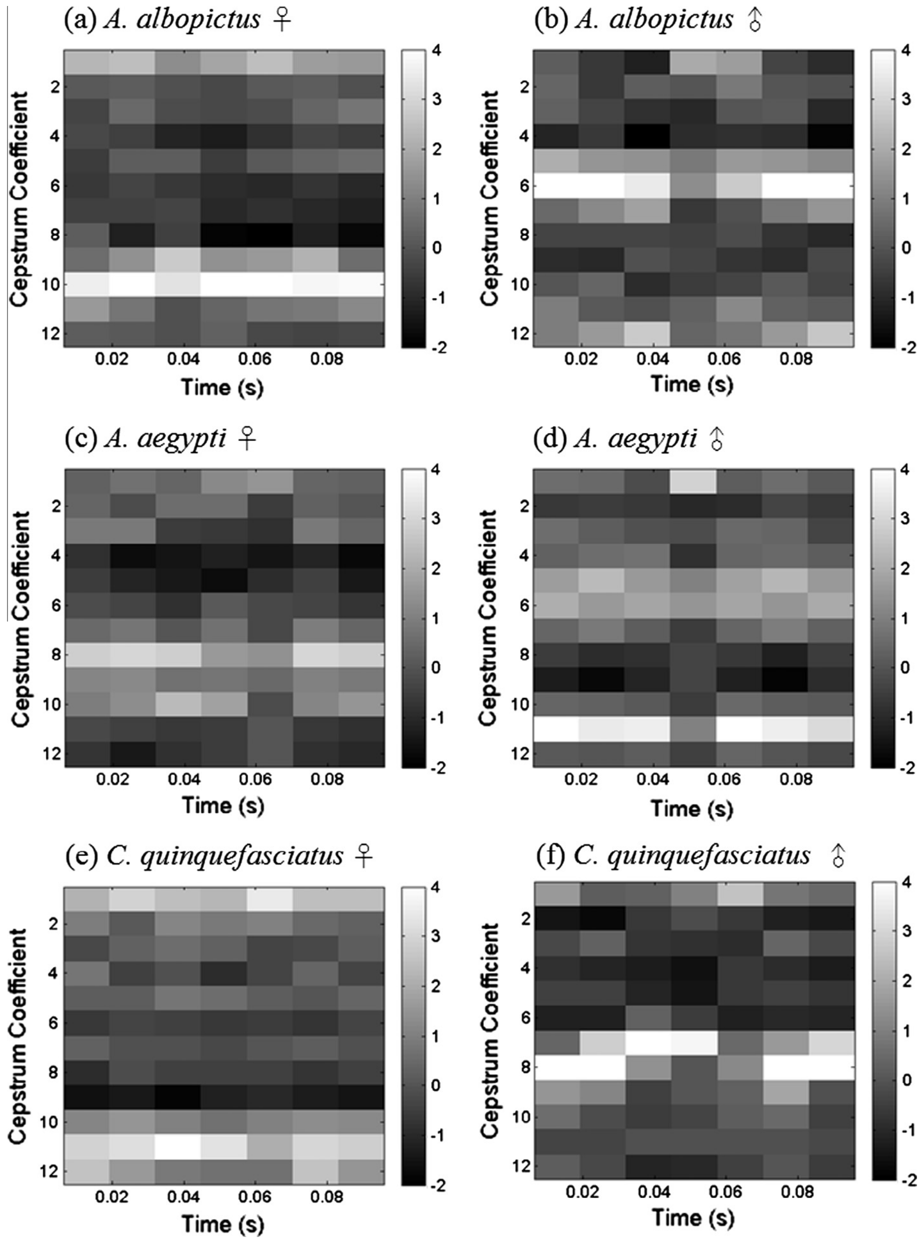

Fig. 3. Typical examples of extracted cepstrograms and time-domain waveforms of 6 groups of mosquitoes tested in the experiments. The cepstrograms are on the left side of each subfigure; the time-domain waveforms are on the right side.

Table 1
The *p*-values of each two groups yielded from a Two-way ANOVA. The CQ, AA, and AE represent *C. quinquefasciatus*, *A. albopictus* and *A. aegypti*, respectively. The gender symbols ♂ and ♀ denote male and female, respectively. The *p*-value of the pair of *male C. quinquefasciatus – Aedes albopictus* is higher than 0.05, which suggests that the differences in this group might not be significant.

Groups	CQ♀ CQ♂	CQ♀ AA♂	CQ♀ AE♂	CQ♀ AA♀	CQ♀ AE♀	CQ♂ AA♂	CQ♂ AE♂	CQ♂ AA♀	CQ♂ AE♀	AA♂ AA♀	AA♂ AA♀	AA♂ AE♀	AE♂ AA♀	AE♂ AE♀	AA♀ AE♀
p-value	0	0	0	0	0	0.1367	0.0001	0.0097	0	0.0121	0	0	0	0	0.0081

($p > 0.05$), which implies that it is challenging to classify two groups that share similar wingbeat characteristics when solely relying on the wingbeat cepstrum characteristics. According to the previous studies, the variances of the waveform amplitude and frequency might be caused by the variances of size, flight speed within the species, and the environmental conditions (Reed et al., 1942; Rueda et al., 1990; Mankin, 1994; Briegel et al., 2001; Ptitsyn et al., 2011), and the relations of wingbeat frequency patterns to wing loading, wing shape, and body mass (Ellington, 1984; Byrne et al., 1988). Moreover, the overlapped ranges of wingbeat frequencies and patterns have been presented and studied (Mankin, 1994; Göpfert and Robert, 2001; Gibson and Russell, 2006; Cator et al., 2009; Pennetier et al., 2010). The variances of wingbeat characteristics could be attributed to mosquitoes' wingbeat changes, and could be treated as communication measures for courtship and species recognition (Gibson and

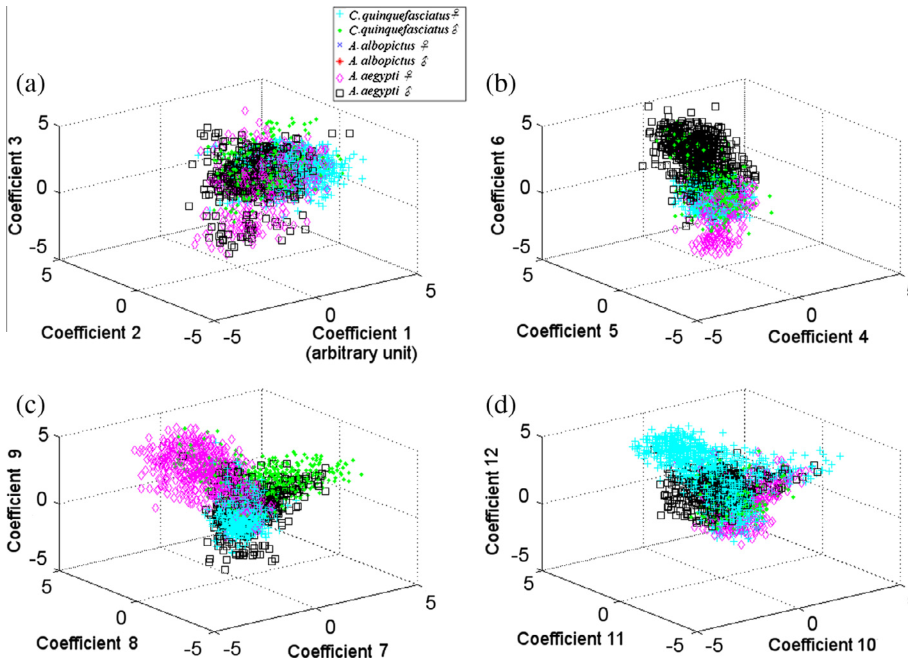

Fig. 4. The scatter plots of 12 coefficients of cepstra from all samples of 6 test groups. (a) The scatter plot that shows the 1, 2, 3 coefficients, (b) the scatter plot that shows the 4, 5, 6 coefficients, (c) the scatter plot that shows the 7, 8, 9 coefficients, and (d) the scatter plot that shows the 10, 11, 12 coefficients.

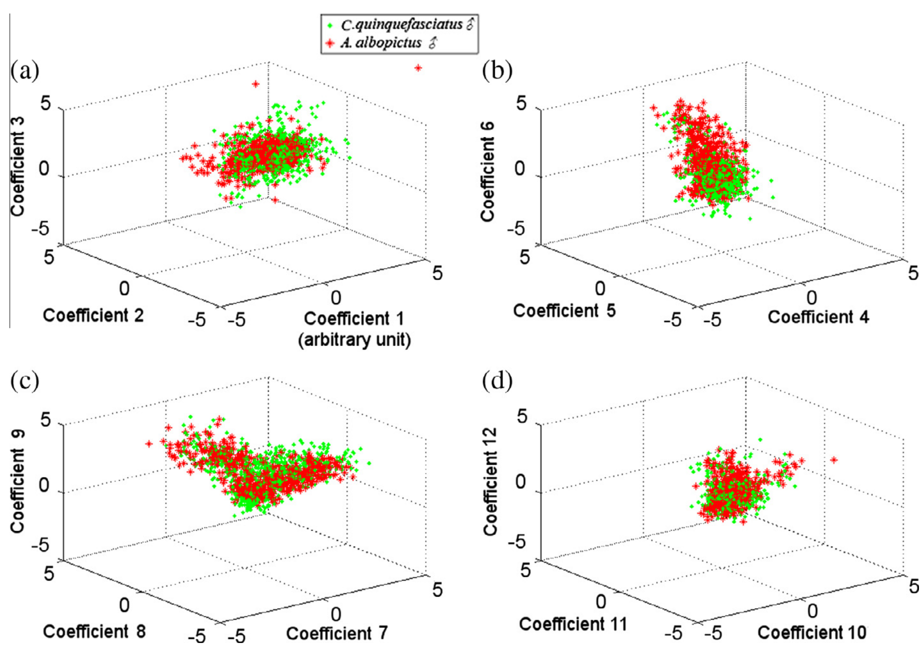

Fig. 5. The scatter plots of 12 coefficients of cepstra from all samples of male *A. albopictus* and male *C. quinquefasciatus* test groups. The distributions of the two groups are similar corresponding to the results of the ANOVA test. (a) The scatter plot that shows the 1, 2, 3 coefficients, (b) the scatter plot that shows the 4, 5, 6 coefficients, (c) the scatter plot that shows the 7, 8, 9 coefficients, and (d) the scatter plot that shows the 10, 11, 12 coefficients.

Russell, 2006; Cator et al., 2009; Pennetier et al., 2010). For example, the courtship behavior through shifting flight tones (Cator et al., 2009) increases the overlapped ranges and the shifting variances of mosquito wingbeat frequencies, which may affect the classification performance of the methods based on the wingbeat characteristics. It is a very challenging task to classifying multiple insect species with the overlapped characteristics due to the biodiversity as well as the degree of freedom of the behavior.

3.3. Comparison of the EM-GMM, ANN, and NN classification methods

As shown in Tables 2–4, the ANN method provides the consistently inferior classification results as well as longer computation time during the training phase compared to the EM-GMM method. The high computational complexity might be a drawback if the system requires an in-field model training phase for the target class of insects. The training and classification time may become

Table 2
A comparison of the performance between the EM-GMM method and ANN method. The confusion matrix presents the results of the gender classification using the three methods, in which each row presents the actual class of the subjects as well as each column presents the predicted class.

Approach	EM-GMM		ANN		Nearest neighbor	
Predicted class Actual class	♂	♀	♂	♀	♂	♀
♂	261	82	244	99	299	44
♀	8	394	5	397	103	299
True positive	261	394	244	397	299	299
False positive	8	82	5	99	103	44
True negative	394	261	397	244	299	299
False negative	82	8	99	5	44	103
Accuracy (%)	87.9		86.0		80.3	
Precision (%)	97.0	82.8	98.0	80.0	74.4	87.2

longer when more neurons and layers are used (Moore and Miller, 2002; Li et al., 2005). Regarding the NN method, although the computational complexity of it is lower than that of the EM-GMM method, its accuracy and precision on classifying the gender, genus, and sex-species classes are worse than those of the EM-GMM method. Therefore, we propose that the EM-GMM method is an optimal method for mosquito classification using the optical sensing device.

Regarding the applicability of the system, the EM-GMM method outperforms the previous methods even when the coefficients of the cepstrum are reduced to 12, which is beneficial when applying the method to embedded systems because of the simplicity compared to the methods which requires hundreds of coefficients. Therefore, the classification results of the gender of the mosquitoes (Table 2) and the between-genus (*Aedes* and *Culex*) results (Table 3) both suggest that the system may satisfy the specifications of a mosquito classification system which is applicable to population monitoring and early-stage warning of a specific epidemic vector.

Additionally, the miniaturized system can be integrated into nodes in wireless sensor network systems for large-scale field environment monitoring, such as ecological studies and pandemic vector population monitoring. With the advantage of detecting the population changes within a few seconds, the optical mosquito classification method proposed in the research is an potential alternative to the ovitraps which are conventionally used in vector monitoring (Fay and Perry, 1965; Zeichner and Perich, 1999; Lenhart et al., 2005) to reduce the delay of detecting an epidemic disease outbreak at an early stage. To develop a robust system with the improved classification capability, an automatic recording segmentation approach can be used to further improve the accuracy of the system by preventing the wingbeat characteristics from being lost during sequences trimming. The analyses of the biological and the environmental factors which cause the variances of overlaps of wingbeat characteristics may be included in further investigations. The biological factors, including the varied size and age, may increase the variance of the estimated mosquito model when the size of the training set is limited, and thus undermine the accuracy. To calibrate the model by addressing the biological factors, one may perform the experiments with a few large sets of the highly homogeneous cohorts of mosquitoes, which are precisely selected by the body size or age of interest to further calibrate the model. The homogeneity of the cohorts may reduce the estimated variances of the model and increase the accuracy and precision of classification, and thus validate if the wingbeat patterns of certain mosquitoes are truly overlapped. For the effect of the environmental factors, one may perform a set of experiments with different setups of the environment factors which may present in the practical applications, including the lighting, the pose of the apparatus, and the temperature. The analysis of the recordings from these setups may answer if the changes of the environmental factors undermine the performance and validate the applicability of the system for practical applications.

3.4. Instrument design

Using the infrared sensor array recording device proposed in this research, the mosquito wingbeat could be recorded and analyzed to build the models for species and gender classification. The recording device has advantages in wingbeat sequence collection. One merit is its robustness in regard to acoustic noise, which is difficult to avoid when applying the system to field monitoring. The simplicity of the mechanical structure of the recording device is another merit. This is critical for reducing the costs of manufacturing and maintenance. In addition, the availability of electronic parts used in the device is high, because the infrared transmitter and receiver pairs in the optical recording device are widely used in infrared remote control for home appliances, costing about US $ 0.3 each pair. Furthermore, the recording device could be conveniently attached to the mosquito traps adopted by the Centers for Disease Control (CDC) in Taiwan for field population monitoring. Although the waveform variances of the mosquito wingbeat sequences may be caused by the different orientations of the wings

Table 3
The confusion matrix that shows the inter-genus and gender classification results for *A. aegypti* and *C. quinquefasciatus*.

Approach		EM-GMM				ANN				Nearest Neighbor			
Predicted class		*Aedes*		*Culex*		*Aedes*		*Culex*		*Aedes*		*Culex*	
Actual class		♂	♀	♂	♀	♂	♀	♂	♀	♂	♀	♂	♀
Aedes	♂	155	36	24	3	157	41	7	13	178	25	12	3
	♀	0	194	2	24	4	161	1	54	56	112	37	15
Culex	♂	29	31	53	12	51	38	29	7	78	16	31	0
	♀	6	29	0	147	0	131	0	51	10	148	0	24
True positive		155	194	53	147	157	161	29	51	178	112	31	24
False positive		35	96	26	39	55	210	8	74	144	189	49	18
True negative		492	429	594	1269	472	315	612	1234	383	336	571	1290
False negative		63	26	72	35	61	59	96	131	40	108	94	158
Accuracy (%)		86.8	83.6	86.8	95.0	84.4	63.9	86.0	86.2	75.3	60.1	80.8	88.2
Precision (%)		81.6	66.9	67.1	79.0	74.1	43.4	78.4	40.8	55.3	37.2	38.8	57.1
Ave. accuracy (%)		88.1				80.1				76.1			
Ave. Precision (%)		73.6				59.2				47.1			

Table 4
The classification results of the six groups in the experiments.

Approach		EM-GMM						ANN						Nearest Neighbor					
Predicted class		*A. aegypti*		*A. albopictus*		*C. quinque-fasciatus*		*A. aegypti*		*A. albopictus*		*C. quinque-fasciatus*		*A. aegypti*		*A. albopictus*		*C. quinque-fasciatus*	
Actual class		♂	♀	♂	♀	♂	♀	♂	♀	♂	♀	♂	♀	♂	♀	♂	♀	♂	♀
A. aegypti	♂	97	12	4	1	6	3	96	16	0	2	2	7	21	6	83	8	2	3
	♀	0	100	0	15	2	5	4	88	0	6	1	23	41	14	0	30	30	7
A. albopictus	♂	48	23	6	0	18	0	61	19	0	4	5	6	56	5	18	6	10	0
	♀	0	62	0	17	0	19	0	44	0	23	0	31	15	26	0	42	7	8
C. quinquefasciatus	♂	29	29	0	2	53	12	51	30	0	8	29	7	72	3	6	13	31	0
	♀	6	7	0	22	0	147	0	72	0	59	0	51	10	33	0	115	0	24
True positive		97	100	6	17	53	147	96	88	0	23	29	51	21	14	18	42	31	24
False positive		83	133	4	40	26	39	116	181	0	79	8	74	194	73	89	172	49	18
True negative		539	490	646	607	594	524	506	442	650	568	612	489	428	550	561	475	571	545
False negative		26	22	89	81	72	35	27	34	95	75	96	131	102	108	77	56	94	158
Accuracy (%)		85.4	79.2	87.5	83.8	86.8	90.1	80.8	71.1	87.2	79.3	86	72.5	60.3	75.7	77.7	69.4	80.8	76.4
Precision (%)		53.9	42.9	60	29.8	67.1	79.0	45.3	32.7	NA	22.5	78.4	40.8	9.8	16.1	16.8	19.6	38.8	57.1
Ave. accuracy (%)		85.5						79.5						73.4					
Ave. precision (%)		55.5						43.9						26.4					

during flying, the fundamental frequency may not be affected (Moore and Miller, 2002; Li et al., 2005). The mechanical design of the recording device proposed in this paper covers the constrained field of measurement so that the interference from the environment is minimized. Furthermore, the double helix arrangement of transmitter and receiver pairs extends the time of recording the wingbeat during flight. The duration of wingbeat varies from 30 ms to more than 200 ms, and the voltage range also varies (Fig. 3). These may make the time-domain feature extraction a challenging task. Previous research also suggested that time-domain wingbeat sequences are not appropriate for inter-specific classification (Moore and Miller, 2002; Li et al., 2005). Therefore, the classification results based on the time-domain waveforms are not included in this research. The cepstral wingbeat distributions of each species shown in Fig. 3 demonstrate the frequency distribution characteristics of each species of mosquito wingbeat. For example, the cepstrogram of male *C. quinquefasciatus* shows a higher frequency distribution than female *C. quinquefasciatus,* which implies that the frequency distribution could be further investigated (Moore and Miller, 2002).

4. Conclusions

In this study, we proposed a recording device which consists of an optical sensor array for the acquisition of mosquito wingbeat sequences and a set of machine learning methods for modeling the mosquito wingbeats and group classification.

To identify the optimal machine learning method, we performed the experiments using living subjects, and compared the performances of the methods for classification of the groups of mosquitoes. The statistical analyses on the results suggest that the EM-GMM method is superior to the other methods on the accuracy of classifying the subjects' genus and gender.

In the wingbeat characteristics of certain groups of mosquitoes, we found that the cepstra of the six groups of the mosquitoes are significantly different from each other except that the wingbeat patterns of male *C. quinquefasciatus* and male *A. Albopictus* are similar to each other. This discrepancy implies that it might not be feasible to differentiate the wingbeat patterns between the two groups, and thus explains the suboptimal performance of the classification of them.

Compared with the performance evaluation results provided by the previous studies that identify insects based on their wingbeat characteristics, the system that we proposed in this study is advantageous because of its superior accuracy and efficiency on classification and robustness with regard to the acoustic noises in the environment. For the practical applicability of the system for disease vector monitoring and agricultural research, the simplicity of the system for manufacturing, maintenance, and the low computational requirement for the embedded system address the concerns about the cost and the reliability in the scenario of massive deployment of the system in the field.

References

Atal, B.S., 1974. Effectiveness of linear predication characteristics of the speech wave for automatic speaker identification and verification. J. Acoust. Soc. Am. 55 (6), 1304–1312.

Belton, P., Costello, R.A., 1979. Flight sounds of the females of some mosquitoes of Western Canada. Entomol. Exp. Appl. 26 (1), 105–114.

Briegel, H., Knüsel, I., Timmermann, S.E., 2001. *Aedes aegypti*: size, reserves, survival, and flight potential. J. Vec. Ecol. 26 (1), 21–31.

Byrne, D.N., Buchmann, S.L., Spangler, H.G., 1988. Relationship between wing loading, wingbeat frequency and body mass in homopterous insects. J. Exp. Biol. 135, 9–23.

Cator, L.J., Arthur, B.J., Harrington, L.C., Hoy, R.R., 2009. Harmonic convergence in the love songs of the dengue vector mosquito. Science 323 (5917), 1077–1079.

Chadwick, L.E., 1939. A simple stroboscopic method for the study of insect flight. Psyche 46 (1), 1–8.

Dempster, A.P., Laird, N.M., Rubin, D.B., 1977. Maximum likelihood from incomplete data via the EM algorithm. Statist. Soc. Ser. B Metho. 39 (1), 1–38.

Ellington, C.P., 1984. The aerodynamics of hovering insect flight. III. Kinematics. Phil. Trans. B 305, 41–78.

Eritja, R., Escosa, R., Lucientes, J., Marquès, E., Roiz, D., Ruiz, S., 2005. Worldwide invasion of vector mosquitoes: present European distribution and challenges for Spain. Biol. Invasions 7 (1), 87–97.

Fay, R.W., Perry, A.S., 1965. Laboratory studies of ovipositional preferences of *Aedes aegypti*. Mosq. News 25, 276–281.

Gauvain, J.L., Lee, C.H., 1994. Maximum *a posteriori* estimation for multivariate Gaussian mixture observations of Markov chains. IEEE Trans. Speech Audio Proc. 2 (2), 291–298.

Gibson, G., Russell, I., 2006. Flying in tune: sexual recognition in mosquitoes. Curr. Biol. 16, 1311–1316.

Gish, H., Schmidt, M., 1994. Text-independent speaker identification. IEEE Signal Process Mag. 11 (4), 18–32.

Göpfert, M.C., Robert, D., 2001. Active auditory mechanics in mosquitoes. Proc. Biol. Sci. 268 (1465), 333–339.

Gubler, D.J., 1989. *Aedes Aegypti* and *Aedes Aegypti*-borne disease control in the 1990s: top down or bottom up. Am. J. Trop. Med. Hyg. 40 (6), 571–578.

Gubler, D.J., Clark, G.G., 1996. Community involvement in the control of *Aedes aegypti*. Acta Trop. 61, 169–179.

Hardie, J., Powell, G., 2002. Video analysis of aphid flight behavior. Comput. Electron. Agric. 35, 229–242.

Ikawa, T., Okabe, H., Mori, T., Urabe, K., Ikeshoji, T., 1994. A method for reconstructing three-dimensional positions of swarming mosquitoes. J. Insect Behav. 7 (2), 237–248.

Jackson, J.C., Robert, D., 2006. Nonlinear auditory mechanism enhances female sounds for male mosquitoes. Proc. Natl. Acad. Sci. 103 (45), 16734–16739.

Johnston, C., 1855. Auditory apparatus of the *Culex* mosquito. Quart. J. Microsc. Sci. 3, 97–102.

Jones, M.D.R., 1964. The automatic recording of mosquito activity. J. Ins. Physiol. 10 (2), 349–351.

Kinnunen, T., Karpov, E., Franti, P., 2006. Real-time speaker identification and verification. IEEE Trans. Audio Speech Lan. Process. 14 (1), 277–287.

Landois, H., 1867. Die ton- und stimmapparate der insekten in anatomisch-physiologischer und akustischer beziehung. Zeitschrift für Wissenschaftliche Zoologie 17, 105–184.

Lenhart, A.E., Walle, M., Cedillo, H., Kroeger, A., 2005. Building a better ovitrap for detecting *Aedes aegypti* oviposition. Acta Trop. 96 (1), 56–59.

Li, Z.Y., Zhou, Z.J., Shen, Z.R., Yao, Q., 2005. Automated identification of mosquito (Diptera: Culicidae) wingbeat frequencies by artificial neural network. Artif. Intell. Appl. Innov. 187, 483–489.

Mankin, R.W., 1994. Acoustical detection of *Aedes taeniorhynchus* swarms and emergence exoduses in remote salt marshes. J. Am. Mosquito Contr. 10 (2), 302-208.

Moore, A., 1991. Artificial neural network trained to identify mosquitoes in flight. J. Insect Behav. 4 (3), 391–396.

Moore, A., Miller, R.H., 2002. Automated identification of optically sensed *Aphid* (*Homoptera: Aphidae*) wingbeat waveforms. Ann. Entomol. Soc. Am. 95 (1), 1–8.

Moore, A., Miller, J.R., Tabashnik, B.E., Gage, S.H., 1986. Automated identification of flying insects by analysis of wingbeat frequencies. J. Econ. Entomol. 79 (6), 1703–1706.

Oertli, J.J., 1989. Relationship of wing beat frequency and temperature during take-off flight in temperate-zone beetles. J. Exp. Biol. 145, 321–338.

Pennetier, C., Warren, B., Dabire, K.R., Russell, I.J., Gibson, G., 2010. ''Singing on the Wing'' as a mechanism for species recognition in the malarial mosquito *Anopheles gambiae*. Curr. Biol. 20 (2), 131–136.

Polson, K., Curtis, C., Seng, C.M., Olson, J.G., Chantha, N., Rawlins, S.C., 2002. The use of ovitraps baited with hay infusion as a surveillance tool for *Aedes aegypti* mosquitoes in Cambodia. Dengue Bulletin 26, 178–184.

Ptitsyn, A.A., Reyes-Solis, G., Saavedra-Rodriguez, K., Betz, J., Suchman, E.L., et al., 2011. Rhythms and synchronization patterns in gene expression in the *Aedes aegypti* mosquito. BMC Genomics 12, 153.

Reed, S.C., Williams, C.M., Chadwick, L.E., 1942. Frequency of wing-beat as a character for separating species races and geographic varieties of *Drosophila*. Genetics 27 (3), 349–361.

Reynolds, A., 1995. Speaker identification and verification using Gaussian mixture speaker models. Speech Comm. 17 (1), 91–108.

Reynolds, D.A., Rose, R.C., 1995. Robust text-independent speaker identification using Gaussian mixture speaker models. IEEE Trans. Speech Audio Process. 3 (1), 72–83.

Reynolds, D.R., Riley, J.R., 2002. Remote-sensing, telemetric and computer-based technologies for investigating insect movement: a survey of existing and potential techniques. Comput. Electron. Agric. 35, 271–307.

Riley, J.R., 1989. Remote sensing in entomology. Ann. Rev. Entomol. 34, 247–271.

Riley, J.R., Smith, A.D., 2002. Design considerations for an harmonic radar to investigate the flight of insects at low altitude. Comput. Electron. Agric. 35, 151–169.

Robert, D., 2009. Insect bioacoustics: mosquitoes make an effort to listen to each other. Curr. Biol. 19 (11), 446–449.

Rueda, L.M., Patel, K.J., Axtell, R.C., Stinner, R.E., 1990. Temperature-dependent development and survival rates of *Culex quinquefasciatus* and *Aedes aegypti* (*Diptera: Culicidae*). J. Med. Entomol. 27, 892–898.

Sotavalta, O., 1952. Flight-tone and wing-stroke frequency of insects and the dynamics of insect flight. Nature 170, 1057–1058.

Unwin, D.M., Ellington, C.P., 1979. An optical tachometer for measurement of the wing-beat frequency of free-flying insects. J. Exp. Biol. 82, 377–378.

Williams, C., Galambos, M.R., 1950. Oscilloscopic and stroboscopic analysis of the flight sounds of *Drosophila*. Biol. Bulletin 99 (2), 300–307.

Zeichner, B.C., Perich, M.J., 1999. Laboratory testing of a lethal ovitrap for *Aedes aegypti*. Med. Vet. Entomol. 13 (3), 234–238.